HHS Public Access

Author manuscript

J Control Release. Author manuscript; available in PMC 2018 September 28.

Published in final edited form as:

J Control Release. 2017 September 28; 262: 201–211. doi:10.1016/j.jconrel.2017.07.029.

Reshapable polymeric hydrogel for controlled soft-tissue expansion: *In vitro* and *In vivo* evaluation

John Garner[1], **Darrel Davidson**[2], **George J. Eckert**[3], **Clark T. Barco**[4], **Haesun Park**[1], and **Kinam Park**[1,5]

[1]Akina, Inc. West Lafayette, IN

[2]Department of Pathology and Laboratory Medicine, Indiana University School of Medicine, Indianapolis, IN

[3]Department of Biostatistics, Indiana University School of Medicine, Indianapolis, IN

[4]Roudebush Veterans Affairs Medical Center, Indianapolis, IN

[5]Purdue University, Departments of Biomedical Engineering and Pharmaceutics, West Lafayette, IN

Abstract

Tissue expansion is the process by which extra skin is generated using a device that applies pressure from underneath the skin. Over the course of weeks to months, stretching by this pressure creates a flap of extra tissue that can be used to cover a defect area or enclose a permanent implant. Conventional tissue expanders require a silicone shell inflated either by external injections of saline solution or air, or by internal osmotic pressure generated by a hydrophilic polymer. In this study, a shell-free tissue expander comprised only of a chemically cross-linked biocompatible polymeric hydrogel is developed. The cross-linked network of hydrophilic polymer provides for intrinsically controlled swelling in the absence of an external membrane. The new type of hydrogel expanders were characterized *in vitro* as well as *in vivo* using a rat-skin animal model. It was found that increasing the hydrophobic polyester content in the hydrogel reduced the swelling velocity to a rate and volume that eliminate the danger of premature swelling rupturing the sutured area. Additionally, increasing the crosslinking density resulted in enough mechanical strength of the hydrogel to allow for complete post-swelling removal, without the hydrogel cracking or crumbling. No systemic toxicity was noted with the expanders and histology showed the material to be highly biocompatible. These expanders have an advantage of tissue expansion without requiring an external silicone membrane, and thus, they can be cut or reshaped at the time of implantation for applications in small or physically constrained regions of the body.

Graphical abstract

Corresponding Author: Kinam Park, Ph.D., Akina, Inc., 3495 Kent Avenue, West Lafayette, IN 47906, pk@akinainc.com.

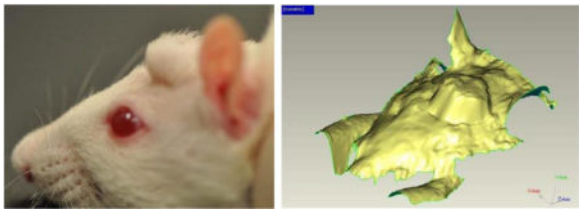

Keywords

Tissue expander; cross-linked hydrogels; reshapable; poly(ethylene glycol) diacrylate; poly(lactic-co-glycolic acid); PLGA-PEG-PLGA

1. Introduction

Tissue expanders are an important tool for generating extra skin for use in reconstructive surgery. Tissue expanders have a long history of successful use in clinical applications, dating back to 1957, to expand skin and support tissues by applying pressure underneath the dermis [1–4]. When a part of the human body is lost or damaged, tissue expanders are used to increase the amount of soft tissue in preparation for replacement of tissues lost [5]. For example, a tissue expander can be used to increase the oral mucosa for a significantly more predictable bone graft, developing for a subsequent dental implant. Moreover, new tissue created by a tissue expander may be used for subsequent reconstructive surgical procedures, such as inserting a breast prosthesis following mastectomy, or replacing skin lost to a burn. Tissue expanders are often used in various locations including the chest wall, head, neck, shoulder, arm, ear, finger, hairline, lower-back, groin, calf and foot regions [6–12].

Currently, the majority of tissue expanders are essentially silicone elastomer balloons surgically placed under the skin and inflated over the course of several weeks of healing. This inflation is usually done by injecting sterile saline into the balloon. Finding portals for this periodic fluid injection is difficult, time-consuming, and the process is painful for the patient. The overall design of expanders has changed little over the years. Most tissue expanders are basically subcutaneous bags that are externally inflated at timed intervals [13–16]. There are significant drawbacks to this design, especially the need of multiple injections and interventions into the same location can increase the risk of infection or hemorrhage [17]. The use of inflatable balloons also sets a lower limit on the size or shape of expanders.

“Self-swelling” Hydrogel tissue expanders provide a way to avoid this periodic injection of fluid for expansion. Several hydrogel tissue expanders have already been developed. All of them, however, are enclosed inside a silicone rubber shell to control the rate of expansion and to avoid tearing the wound within the first weeks following surgical placement [18–24]. The presence of a silicone rubber shell restricts the application of commercial hydrogel expanders to a limited number of sizes and shapes. Due to this limitation, hydrogel tissue expanders have not been applied for applications which require small expanders of exact size for specific locations [25]. The purpose of this research is to develop a self-swelling, hydrogel tissue expander that can be reshaped using scissors or a knife at the time of emplacement by a surgeon. This self-swelling and reshapable tissue expander can overcome

problems associated with current technology by eliminating exterior equipment and allowing custom fitting of the expander to the tissue by the surgeon.

Poly(lactide-co-glycolide) (PLGA) is a hydrophobic, biodegradable polyester which has been used for decades both in mechanical applications, such as sutures [26], and a wide variety of drug-delivery applications [27]. PLGA naturally hydrolyzes to non-toxic components, lactic acid and glycolic acid [28]. Poly(ethylene glycol) (PEG) is a non-degradable, hydrophilic polyether which has good biocompatibility, as it elicits little immune response [29]. PLGA and PEG were utilized to prepare hydrogels with controllable swelling properties. The swelling of the non-degradable, hydrophilic PEG is modified by the hydrolysis rate of degradable PLGA so that the swelling of the entire structure can be controlled.

This study investigates a new shell-free, reshapable hydrogel by *in vitro* and *in vivo* testing. This device is designed to expand skin at a controlled rate without over-expansion that may cause eruption through the incision or ischemia and necrosis of overlying tissue. Furthermore, it is desirable for such an expander to be reshaped at the time of emplacement to match the void size and shape. This would allow for tissue expansion in tight or constrained regions where traditional expanders do not fit.

2. Materials and methods

2.1. Materials

Acryloyl chloride (AAc), triethylamine (TEA), poly(ethylene glycol) diacrylate (PEGDA), ethylene glycol dimethacrylate (EGDMA), azobisisobutyronitrile (AIBN), and stannous octoate (SnOct) were obtained from Sigma Aldrich. SnOct was purified by vacuum distillation prior to usage. AIBN was purified by recrystallization from methanol and stored frozen. Triethylamine (TEA) was vacuum distilled and stored over KOH. Dichloromethane (DCM) and hexane were obtained from Malinckrodt. Poly(lactic-co-glycolic acid) (PLGA, Cat.No. RG503H) was obtained from Boeinger Ingelheim. Other reagents were of analytical quality and used as received.

2.2. Synthesis and characterization of tissue expander polymers

Triblock PLGA-PEG-PLGA diacrylate was synthesized as previously described [30–32]. Briefly, a PEG-diol of required molecular weight was obtained commercially (Sigma Aldrich) and dried under deep vacuum in a round bottom flask with stirring at 150 °C for 4 hours to remove water. The dehydrated PEG-diol was back-flushed with inert argon and DL-lactide and glycolide monomers were added to the PEG. As a catalyst, SnOct dissolved 10% w/v in toluene was added in a ratio of 1/200 mole catalyst/monomers. These were placed under a deep vacuum for 0.5 hour, sealed off, and then heated to 150 °C for 8 hours.

PLGA-PEG-PLGA with a wide variety of block sizes was generated using this method by controlling monomer to initiator ratio. The alcohol endcaps of the PEG-diol serve as the initiator of this system. As such, the molar ratio of PLGA monomers to PEG block controls the relative molecular weights of the resultant PLGA-PEG-PLGA block copolymer. For example, PLGA-PEG-PLGA (5000-1000-5000 Da, 50:50 lactide:glycolide (L:G)) was

obtained by reacting 10 grams of PEG diol (1000 Da, 0.01 moles) with 55.4 g DL-lactide (0.38 moles) and 44.6 g glycolide (0.38 moles) catalyzed by 15.6 ml of 10% SnOct/toluene. By carefully selecting reaction feed ratios, the resultant triblock block weight could be controlled [33]. Additionally, PLA and PLGA dialcohol polymers were generated by replacing the PEG block with 1,10-decanediol and performing the same reaction without the initial dehydration step [34]. After synthesis, the crude polymer was dissolved in a small amount of dichloromethane, filtered and reprecipitated in a mixture of hexane:ethanol (80:20). The resulting filtrate was vacuum dried to obtain the purified PLGA-PEG-PLGA, poly(lactic acid)-diol (PLA-diol), or PLGA-diol product [35].

The polymers were then vinyl activated by acryloyl chloride, converting them to macromers [36, 37]. For this process, the polymer was dissolved in anhydrous DCM with stirring. A 3X molar equivalent, to hydroxyl units, of triethylamine and acryloyl chloride was added to the stirring reaction solution at room temperature. Due to acryloyl chloride's rapid degradation in the presence of water, care was taken to avoid moisture during this process. Due to the dangers associated with acryloyl chloride, the reaction was performed carefully under an externally ventilated fume hood. The flask was fitted with a condenser operated by a recirculating chiller (Neslab RTE-7, Thermo-Scientific) filled with a 1:1 water:ethylene glycol mixture at −10 °C. Atop this, a calcium sulfate (DrieRite) desiccant trap was fitted to prevent backflow of humidity. The flask was heated to 80 °C for two hours under these reflux conditions and subsequently stirred at room temperature overnight. The resultant acrylated polymer was passed through a filter paper to remove triethylamine-HCl and precipitated in an 80:20 hexane:ethanol mixture. Subsequently, it was further purified to remove residual acrylic acid which is poorly removed by conventional precipitation. For this, the polymer was dissolved in dichloromethane and dialyzed against acetonitrile using a regenerated cellulose dialysis membrane (Spectrapor) with a molecular weight cutoff below that of the macromer. Alternatively, the polymer dissolved in ethyl acetate was mixed overnight with activated carbon and filtered. After either of these processes, the purified polymer solution was reduced under vacuum, redissolved in DCM and precipitated once more in 80:20 hexane:ethanol mix.

The polymers were characterized by gel-permeation chromatography (GPC) and proton nuclear magnetic resonance (NMR) spectroscopy. NMR was performed in deuterated chloroform on a 500 MHz instrument by Purdue Interdepartmental NMR Faculty. Fourier-transform infrared spectrophotometry (FTIR) was performed using a Thermo-Matsen Satellite IR system. GPC was performed with DCM as the mobile phase, 1 ml/min against a series of 3 GPC columns (7.8 × 300 mm, mixed porosities) using polystyrene standards (Agilent EasiCal™ standards) to generate a standard curve. This size assay was performed with either a Varian Prostar HPLC system with UV/Vis detection at 235 nm or with a Waters Breeze-2 HPLC system with detection by refractive index.

The purified, vinyl-functionalized macromers were dissolved in anhydrous DMSO. Commercially available macromers, such as PEGDA, and short-chain crosslinkers, such as EGMA, were added in DMSO solution for a total concentration of 10–30% weight per volume (formulations shown in Table 1). AIBN was added to an approximate concentration of 0.04% (w/v) and the solution was degassed by lightly bubbling with argon or

difluoroethane. The resulting combined solution was sealed in a microcentrifuge tube and heated to 65 °C overnight to crosslink. The following day, the microcentrifuge tube top was opened and the bottom was punctured. Compressed difluoroethane applied to the puncture gently pushed the hydrogel out of the microcentrifuge tube. The reshapable hydrogel was soaked for two to three days with shaking in excess ethyl acetate, then soaked in excess ethanol for two to three days to wash away any uncrosslinked components. Marked deswelling of the hydrogel occurred during soaking in solvent-free ethanol. The reshapable hydrogels were then dried under deep vacuum for a week to remove solvents.

Prior to animal experiments, the reshapable hydrogels were sterilized by exposure to ethylene oxide gas either at 54 °C for 16 hours in an Axis AX-60 sterilizer or at room temperature for 24 hours in an Andersen sterilizer. Preliminary tests showed that sterilization by γ-irradiation resulted in a marked decrease in flexibility and in control of swelling (data not shown). This is in accordance with previous results for γ-sterilization of biodegradable systems found by other researchers. γ-irradiation induces a variety of crosslinking and fragmentation reactions within the polymer matrix that alter its properties [38–41].

2.3. *In vitro* Swelling Profile

The hydrogels were shaped by trimming into discs (~3 mm diameter × 2 mm height, dry), weighed dry, and placed in well-plates. To each well, an excess of phosphate buffered saline (PBS, P4417 tablets from Aldrich mixed with DI water per manufacturer's instructions) was added to soak the hydrogel. The hydrogels were incubated at 37 °C in an orbital agitating shaker (MaxQ™ 4450 Benchtop Orbital Shaker, Thermo Fisher Scientific) with agitation at 100 RPM. At predetermined time points, the hydrogel was removed, patted dry with lint-free wipes, and weighed. The swelling ratio was determined as follows:

$$Q_t = \frac{W_t - W_0}{W_0}$$

where Q_t is the swelling ratio at time t and W_t is the weight of the hydrogel at time t and W_o is the weight of the hydrogel at time 0, or the dry hydrogel. The swelling ratio changed over time due not only to swelling of the hydrogel, but also to degradation of the polyester blocks.

2.4. Swelling pressure

Swelling pressure was assayed by placing the reshapable hydrogel disc in a 20 ml scintillation vial on top of a heated stage (37 °C) under the probe arm of a texture analyzer (TA.XT Plus, Texture Technologies, Inc., Hamilton, MA). The texture analyzer tip (1/2-inch Dacron cylinder) was lowered until it touched the hydrogel. The tip was held still at this position while 10 ml of 0.154 M hydrochloric acid (HCl) was added to the vial. HCl was used at an isotonic concentration to represent the same salt content as human biological fluids but in accelerated degradation conditions for a rapid test. The tip was held still while the reshapable hydrogel swelled and the force generated from the swelling of the gel was monitored over 24 hours. The maximum swelling force was divided by the swollen expander contact area to obtain the swelling pressure.

2.5. Mechanical property of dry hydrogels

The cross-sectional area of dry hydrogel discs was measured and the discs were loaded onto the stage of the TA.XT Plus texture analyzer. Each piece was compressed with a ½-inch radius Dacron tip at a crosshead speed of 0.5 mm/sec to 20% strain and held there for 60 seconds and then the tip was withdrawn. The slope of the stress-strain curve from 0–2% strain was measured as the elasticity modulus [42]. The compression force at 20% strain after holding for 60 seconds was divided by the initial compressive force at 20% strain and converted to percent. This was taken as stress relaxation, which is a value related to polymer creep or deformation over time [43].

2.6. Mechanical strength post-degradation

Samples which had undergone a swelling assay for 2 months at 37 °C in PBS were used for post-degradation mechanical strength. For this test, the swollen sample was removed from the well plate and placed on the TA.XTplus platform. It was compressed using a ¼ inch steel ball probe at 0.5 mm/sec. The maximum force obtained (in Newtons) was divided by the disc thickness (in mm) to obtain a relative strength factor for the reshapable hydrogel samples. For this and other *in vitro* tests, the results presented represent an average of at least 3 measurements unless otherwise specified.

2.7. *In vivo* analysis

All work was performed under the auspices of Indiana University School of Medicine Institutional Animal Care and Use Committee (IACUC). All animal testing was performed at the Laboratory Animal Resource Center (LARC) at Indiana University Medical School (IUMed). The reshapable hydrogels selected for animal studies were sterilized and handled aseptically and sterile surgical technique was used for all animal implantations.

Sprague-Dawley rats (~250 gm and 50 days old) were anesthetized by intraperitoneal injection of ketamine (100 to 200 mg/kg), and xylazine (5 to 13 mg/kg). A flap of skin and subcutaneous tissue above the rat's skull was reflected. A 3 mm × 2 mm (diameter × height) disc of the hydrogel was placed beneath the flap on top of the skull and the wound was closed by interrupted sutures (Fig. 1-A). For tracking of the reshapable hydrogel expansion, each rat head was scanned with a 3D scanning Faro arm (FARO, Lake Mary, Florida, USA) three times per week with the rats anesthetized by isoflurane (Fig. 1-B). A red line at the bottom of the sutures in Fig. 1 is the FaroArm® scan moving across the skin over the placed reshapable hydrogel. One limitation of this method is that the scanner only provides a 3D rendering of the external features of the rat head with no details provided regarding the underlying structure or composition. This can affect the apparent size of the measurements.

After 6 weeks of expansion, the rats were sacrificed and the expanders were removed. Histology was performed on tissue cross sections of the calvarial periosteum and skin flap that had surrounded the hydrogel before removal. Grossly, a thin pseudocapsule remained with the skin ellipse so that cross sections were easily made after formalin fixation. Initially this work was performed as a pilot study with 18 rats. As a control, commercially available Osmed™ expanders (Osmed Gmb h, Stuttgart, Germany) were also implanted above the rats' skull.

2.8. Histometric analysis

Immediately after harvesting, the tissue samples were fixed in a neutral 10% solution of formaldehyde in phosphate buffered saline at room temperature. Fixed tissues were cut into 2 mm-thick sections, dehydrated and embedded in paraffin blocks according to laboratory standard procedures. Four-micron sections from each tissue sample were stained with hematoxylin and eosin (H&E), or with Masson's trichrome stain according to standard protocols.

Sections stained with H&E were useful for identifying inflammatory cells and for locating phagocytic histiocytes (foam cells). Trichrome staining was helpful for studying vascularity, identifying residual fragments of hydrogel and measuring the capsule thickness. Residual hydrogels that are usually found in animal studies appear to be blisters or bubbles of faintly blue material pinched off from the main gel body by fibrous tissue of the capsule. These signs of retained hydrogel were, therefore, designated as "blebs." These were scored as either absent or present.

Each histologic feature was graded by three examiners and discrepancies in scoring were resolved by conference review of the relevant sections at a multi-head microscope. Binary acute and chronic inflammation scores indicated either absence or presence of neutrophil or lymphocyte infiltration, respectively. The score was 0 if no more than 3 of the relevant inflammatory cells were found in the section. Foam cells were assumed to represent phagocytosis of foreign material near the hydrogel. Scores were 0 for no foam cells, 1 for fewer than 3 foam cells, 2 for 4~6 foam cells, 3 for clusters of foam cells, and 4 for groups of foam cells seen at low power adjacent to the capsule. Thickness of the fibrous capsule was measured at an area where there was no distortion by oblique tissue orientation or partial thickness sectioning. Scores for capsule were 0 for no fibrous capsule, 1 for capsule thickness ≤20 μm, 2 for 20~50 μm, 3 for 50~100 μm, and 4 for ≥100 μm. Vascularity was assumed to represent either native dermal capillaries or reparative neo-vessels generated by angiogenic cytokines related to surgery or the hydrogel implant. Since these neo-vessels are larger, have no pericytes and are often congested, they are more easily seen at low magnification than normal resident capillaries. Grades for vascularity, therefore, were 0 for small capillaries seen only with the high power objective, 1 for scattered, congested capillaries visible with 10× objective, 2 for increased numbers and clusters of capillaries, 3 for large, irregular, thin-walled venule-like neo-vessels, and 4 for crowded thin-walled vessels with stromal edema surrounding the hydrogel capsule.

3. Results

3.1. Synthesis and characterization of reshapable hydrogels

The new reshapable hydrogel expander developed in this research consists of hydrophilic poly(ethylene glycol) (PEG) block and hydrophobic poly(lactide-co-glycolide) (PLGA) that controls the swelling rate. As previously reported [31, 32], the swelling of the whole polymer matrix is temporarily retarded by the hydrophobic polyester regions, which results in a lag time before the expander starts swelling. Such a lag time is designed for the tissue to heal after surgical implantation of the hydrogel.

A series of custom acrylate activated macromers were synthesized as listed in Table 1. The L:G ratio of PLGA was 50:50, and the molecular weights of PLGA and PEG blocks were also varied from 333 to 7,500 and from 1,000 to 1,500, respectively. M4 in Table 1 was generated by modification of PLGA with acryloyl chloride.

As described, this series of custom crosslinkers were first synthesized to prepare delayed swelling hydrogels. The crosslinkers were made by ring opening polymerization followed by reacting with acryloyl chloride to attach reactive vinyl groups. Fig. 2 shows an NMR spectrum of a custom made PLGA-PEG-PLGA diacrylate crosslinker, and peak assignments of $CDCl_3$ solvent, acrylate, lactide, glycolide, terminal ethylene glycol, polymer ethylene glycol, and lactide methyl groups.

The acrylate content was quantified by proton counting. The sum integration of the peaks from 5.9–6.6 ppm (3.72 in total) is attributed to acrylate vinyl units (3H). This was comparing with the peak integration at 3.6 ppm (52.69) which corresponds to poly(ethylene glycol) (4H per ethylene glycol unit). According to the manufacturer's information, the PEG has an average of approximately 22.7 repeating units (~1000 Da). By comparing the integrations, the acrylate content was quantified as 2.1 acrylates/chain. It is not exactly 2.0, due to dispersity of the polymer chains. It is, however, suitably acrylate activated to serve as a macromer.

FTIR results also confirmed the presence of ester, ether, and acrylate moieties as expected. In the FTIR spectra, strong bands were observed at ~1750 cm^{-1} due to ester bonds. Smaller peaks were seen around 1680 cm^{-1} indicating alkene (C=C) stretching of acrylates and in the 3100 cm^{-1} region indicating alkenyl (C=C−**H**) stretching. There was also a strong C−O stretch band in the 1100 cm^{-1} region from ether bonds of PEG as well as a band around 1200 cm^{-1} from ester and acrylate C-O stretching [44–46]. An example FTIR spectrum is shown in Fig. 3.

GPC was performed to measure the molecular weight of the synthesized macromer components by calibrating the chromatograms using known polystyrene standards. The exact molecular weight values obtained from GPC varied from lot-to-lot, but were generally in good accordance with the expected values based on nominal molecular weights. For example, M2 (5000-1000-5000 Da) has a nominal overall molecular weight of 11,000 Da. Table 2 below shows GPC data from a series of lots of this material. Typically, number average molecular weight tends to run low due to skewing by short-chain components, and weight average molecular weight tends to run higher due to skewing by high molecular weight components [47]. These data support a nominal molecular weight between these values. A ratio of these extreme values, the polydispersity index (PDI), gives an estimate of the molecular mass distribution or size heterogeneity index. As polymer chains approach uniform chain length, the PDI approaches unity (1.00). The macromers listed in Table 1 were used to generate reshapable hydrogels of different properties, as shown in Table 3. The reactions were done in anhydrous DMSO at concentrations between 10–30% (w/v, total solids).

3.2. Swelling Rate

Each reshapable hydrogel was tested for its swelling rate and weight ratio profile by measuring the weight change at predetermined time points in PBS. Swelling of the monolithic hydrogels is assumed to be uniform along all axes (isotropic), and thus, changes in mass due to water absorption would be directly related to the change in size. An interesting feature to the swelling profile was observed upon varying the relative quantities of PEG and polyester content. Fig. 4-A shows a swelling profile of a reshapable hydrogel with a high PEG content. In the beginning, the swelling ratio was limited to about 10, followed by very slow swelling for about a week. The hydrogel started swelling faster and reached a peak swelling ratio of about 130 at Day 14. The rapid increase after 10 days is due to degradation of polyester crosslinks. The sharp decrease after reaching the peak is due to dissolution of PEG molecules after degradation of PLGA crosslinks.

When the reshapable hydrogels were synthesized with a higher quantity of hydrophobic PLGA, the overall swelling decreased. The swelling ratios of Formulation 3 in Fig. 4-B are an order of magnitude smaller than those in Fig. 4-A. The swelling continued at a slow rate, reaching the swelling ratio of 5 after 60 days. For the low PLGA content expanders (e.g., Formulation 1), the degradable hydrophobic chains create temporary crosslinks which hold the structure in place and do not allow the gel expansion until they are cleaved [31]. The material as a whole is highly hydrophilic and once the crosslinks are broken there is extensive swelling prior to complete dissolution. For the high PLGA content expanders (e.g., Formulation 3), expansion is controlled by the presence of crosslinks and the overall increase in hydrophobicity from PLGA. In other prototypes, additional permanent crosslinks were generated by the addition of ethylene glycol dimethacrylate (EGDMA) to the reaction (e.g., Formulation 13). This resulted in a specific maximum swelling ratio based on non-degradable crosslinks. This limit in the maximum swelling allows easy control of the final swelling ratio by the permanent crosslinks (Fig 4-C). It is noted that the plateau swelling ratio of 1.8 was obtained after 30 days. In about 2 weeks, the swelling ratio was around 1.4, indicating 12% expansion in each direction. Fig. 4-D shows the swelling kinetics of the Osmed expander which relies on a hydrogel wrapped inside of a silicone rubber membrane. Small holes in the membrane allow for controlled access to fluids, and the maximum swelling is controlled by the expansion of the silicone rubber membrane. The swelling profile of an Osmed expander shows that the plateau swelling ratio of 3 was reached in about 2 weeks. This is a 44% increase in size in all directions. In a confined environment, a hydrogel with 44% expansion in one dimension may exert more pressure than that with 12% expansion in one dimension. Such a difference may be critical in certain applications, e.g., swelling of a hydrogel implanted under tissue with suturing. One critical difference between reshapable hydrogel formulations made in this study and the Osmed expander is that the swelling of Osmed is controlled by the external silicone rubber membrane, while the reshapable hydrogels synthesized in this study is controlled by the hydrogel itself without any wrapping membrane [18, 48]. Thus, the hydrogel expanders prepared in this study can be reshaped in size by cutting and the swelling kinetics can be controlled by the reshapable hydrogel composition and not by the membrane coating.

3.3. Mechanical Properties/Swelling Pressure

The dry hydrogel for tissue expander applications needs to have mechanical properties allowing for reshaping prior to emplacement. Elastic deformability makes it possible for surgeons to modify the size and shape of the dry hydrogel at the time of insertion. These properties were assayed by compressing discs of the reshapable hydrogel expander using the TA.XTplus mechanical tester. Results from this testing are shown in Table 4. Each hyd rogel example used in the study displayed similar dry mechanical properties suitable for shape modification by typical steel blades during the implantation procedure.

Another key property for tissue expansion applications is the swelling pressure which results from the expanding hydrogel encountering changing physical constraints of the surrounding tissue. Previous research has established a range from 25 to 235 mmHg as an appropriate pressure to elicit tissue expansion [18, 49, 50]. Thus, tissue expanders need to be capable of generating at least 25 mmHg of pressure to expand tissues. To test the swelling pressure, expanders were swollen in an acidified saline immersion between the mechanical tester probe and the bottom of a vial. To expedite the degradation of PLGA crosslinkers, the pH of the physiological saline solution was lowered by adding hydrochloric acid (0.154 M HCl, pH ~ 0.8–1.0) [51, 52]. In this test system the reshapable hydrogel swelling pressures were 2- to 7-fold greater than 235 mmHg, the upper limit of the reported appropriate pressure for tissue expansion. The *in vitro* swelling test indicated that the swelling pressure of the reshapable hydrogels was adequate to expand tissue, and it was anticipated that lower ionic strength and competing tissue oncotic pressure would limit the swelling pressure *in vivo*. However, when the expansion pressure exceeds 235 mmHg it can compress tissue arterioles and reduce blood circulation to the flap. Thus, the swelling pressure alone would reduce blood perfusion [53]. The swelling pressures in Table 4, however, were obtained in an accelerated PLGA degradation condition. Thus, in *in vivo* applications, the delayed, slow swelling is not expected to cause the problem. The *in vivo* tests below address this point.

3.4. Mechanical Strength post-degradation

Clinical use of the expander relies on the fact that it is a temporary implant. After the expander has generated a flap of tissue, it must be removed to make space for the subsequent permanent implant or to use the tissue for closure procedures. The test methodology was adapted from techniques used in the food industry for semi-solid and hydrogel type materials [53–56]. In this case, the force required to press a ¼ inch steel ball through the fully swollen expander was divided by the expander thickness to generate a quantifiable description of the reshapable hydrogels post-swelling mechanical strength (Table 5).

Formulation 1 hydrogel without a non-degradable crosslinker, EGDMA, did not maintain the gel shape and dissolved into a liquid after 16 days of incubation. All formulations in Table 5, except Formulation 1, contained EDGMA, and they maintained the hydrogel shape, although the end-strength varied greatly from 0.02 N/mm to 1.45 N/mm. The improved end-strength proved to be critical for functioning as a tissue expander as described in the *in vivo* data below.

3.5. *In Vivo* Test

Reshapable hydrogels with acceptable dry properties, swelling pressure, swelling rate and strength after swelling proceeded to *in vivo* testing in a rat model. For this test, expanders were cut into discs (~2–3 mm thick × 3–5 mm diameter). These discs were implanted with full-thickness in the rat scalp just above the periosteum of calvarium between the ears. The wound was closed with interrupted sutures. During the study, no rat showed any symptom of systemic toxicity, such as weight loss, loss of appetite, or behavioral changes. One rat implanted with formulation 12 had a local infection, which led to sacrifice and exclusion from the study. One rat displayed a non-expander related skin ulceration caused by rubbing his head on the cage top. This accidental trauma was remedied by moving the food supply to the bottom of the cage. The ulcer soon healed and the animal was included in the study. Other than these complications, none of the animals displayed signs of local reaction, such as inflammation, necrosis, dehiscence, or peri-orbital edema. Each rat's head was scanned using a Faro-arm scanner to render a 3D image of the expander. Three-dimensional (3D) image analysis was performed using Geomagic Qualify software to determine volume and surface area of the expanded portion (Fig. 5). This limitation complicates the precise measurement of the expander under the tissue as the rendering does not indicate the difference between expander, flesh, and skull. For this reason, over the course of healing and tissue relaxation, the size of the expander tends to be underestimated especially under late-stage expansion. Despite this limitation, the technique still provides a relative estimate of total expansion.

Initially, a pilot study was performed using six of the prototype expanders in 18 rats. The volume change was calculated from the Faro data based on the volume at initial insertion according to the equation:

$$\Delta V_t = \frac{V_t}{V_i}$$

where V_i represents the volume of the expander right after initial insertion and V_t represents the volume of the expander at the respective time point. The swelling change was calculated at 2, 14, and 42 days of expansion as shown in Table 6 below. On Day 2, post-operative swelling and hemorrhage had resolved on most animals. Tissue expander hydrogels continued to swell to Day 14, except Formulation 8. Formulations 3, 4, and 5 showed reduced size at Day 42, while Formulation 6 kept swelling. Comparison of Formulations 3~6 in Table 3 indicates that Formulation 6 has non-degradable crosslinker EGDMA and a higher amount of PLGA than others. The presence of a higher amount of hydrophobic PLGA is thought to slow down the crosslinker degradation, resulting in continuous swelling. The plateau swelling by Formulation 7 is likely due to the higher (0.5%) concentration of EGDMA, a non-degradable crosslinker.

Upon necropsy, the expanded gels were observed to have induced the formation of a thin, but discrete, fibrous capsule, attached to reflected skin, a process which is common for implants [57]. Fig. 6-A shows an example of fibrous capsule (as indicated by yellow arrows) surrounding a tissue expander hydrogel. Fig. 6-B shows small resorption of bone

surrounding the swollen hydrogel that occurs by pressure of an expanding gel. This happens with all tissue expanders [58]. Some reshapable hydrogels in this pilot study showed mechanically weak structure which became a soft mush when the fibrous capsules were opened. Since this softening appeared related to crosslinking density, subsequent *in vivo* studies focused on more extensively crosslinked formulations.

The next study, a 72-rat study, focused on expansion and end-condition properties. An additional 5 prototypes were generated and tested in 6 rats per each expander formulation. For each test group, three rats were sacrificed after 4 weeks and the remaining after 6 weeks. As a control, 3 commercially purchased Osmed expanders were implanted and tested in the same manner as the hydrogel expanders over 6 weeks. Similar to the pilot study, Faro scans were collected and the volume change at each time point calculated. Fig. 7 shows volume expansion changes for selected prototypes and the Osmed control. Even though a silicone shell covered the core hydrogel in the Osmed formulation, it still swells very fast in the first few days. This fast swelling was tolerated in the current model, but would present problems for stiffer or slower healing tissues. The slow swelling followed by maintaining a certain swollen state turns out to be important for allowing the sutured area to heal and maintain the expanded space.

The Faro scan data primarily provided basic monitoring of the expander. Clinical functionality is the true result from these studies. No expanders presented signs of necrosis or expulsion indicating that the swelling rate was appropriate. Additionally, the end-condition of the reshapable hydrogel is a critical functional parameter for usability. Notably, higher crosslinked formulations presented a higher capacity for removal as a single piece. Fig. 8 displays an image series which relates to this. Of the second prototype series, only Formulation 13 allowed for consistent removal as a single piece without crumbling or cracking. Fig. 8-A shows the implanted hydrogel swollen over time as shown in Fig. 7. Fig. 8-B shows removal of a swollen hydrogel in its intact form. This is one unique mechanical property of the reshapable hydrogel that allows for easy removal after tissue expansion has been made. The left hydrogel in Fig. 8-C is in the fully swollen state of the same hydrogel before implantation on the right. If the hydrogel does not have enough mechanical strength after swelling, it easily breaks into big pieces, as shown in Fig. 8-D. Even though the weak hydrogel broke during removal through incised skin, there were only a few big pieces which were still easy to remove.

3.6. Histological analysis

In addition to notation of expansion and removal conditions, histology was performed on each rat sacrificed at 4 and 6 weeks to determine the effects of reshapable hydrogel formulations on tissue. After fixation in formalin, the samples were transverse sectioned at 1 mm intervals, embedded in paraffin, thin sectioned at 4 μm thickness and stained with hematoxylin and eosin or Masson’s trichrome stain (Fig 9). The prepared samples were scored by an experienced histologist for the presence of hydrogel blebs, fibrous capsule thickness, chronic inflammation, vascularity, foam cells, and acute inflammation.

Chi-square tests were performed to determine if there were any significant differences among groups for blebs, chronic inflammation, or acute inflammation. Mantel-Haenszel

tests for ordered categorical responses were performed to determine if there were any significant differences among groups for fibrous capsule, vascularity, or foam cell scores. There were no statistically significant differences among groups for blebs (p=0.17), fibrous capsule (p=0.30), chronic inflammation (p=0.30), foam cells (p=0.06) or acute inflammation (p=1.00). This indicated that the formulations had biocompatibility at least as good as the current, clinical Osmed material. Formulation 13 had significantly higher vascularity scores than other groups, indicating superior revascularization of the skin flap at 6 weeks. The formation of the macroscopic capsule was suitable for aiding removal of the piece by allowing the hydrogel to slide easily out of the distinct capsule. The capsule and the hydrogel upon removal at necropsy are shown in Fig. 10.

4. DISCUSSION

One way to eliminate the injection issue is to use a hydrogel expander which swells by absorption of surrounding bodily fluids. In this system, it is osmotic pressure rather than external injection controlling the expander swelling. Such an osmotic system named Osmed™ was developed using a matrix of methyl methacrylate and vinylpyrrolidone. There is no delay factor or crosslinked mechanical strengthening with this hydrogel. Rather, it is encased in a silicone shell with select-sized pores to control bodily fluid influx and to stabilize the matrix for complete removal [18, 59, 60]. This external membrane constrains the size and shape for such expanders, especially in small spaces or for specialized applications. A novel expander in which the swelling delay factor is built into the polymer itself and the dry properties allow it to be cut by the surgeon at time of emplacement would overcome these limitations. Such a device could fit the patient rather than forcing the patient to fit the pre-sized expander.

Initial work toward this goal found that the expansion rate could be controlled by creating a system wherein the crosslinks are held in place by PLGA which is hydrolytically degradable allowing for expansion of the hydrogel after a predetermined delay (Fig. 4-A). However, this system did not have the properties desirable for surgical applications. First, the expansion volume was over 25-fold higher than expedient for surgical applications, which require only 2-to 5-fold expansion. Second, the expander became soft and liquid after the crosslinks degraded making removal impractical. The simple addition of permanent crosslinks using non-degradable (within the usage time scale) EGDMA allowed the expanders to maintain form and have residual strength after the degradable crosslinks had cleaved (Fig. 4-B). Additionally, the incorporation of higher molecular weight PLGA components into the reaction mix allows for dual delay mechanisms in which the delay factor is controlled both by the breaking of crosslinks and by the shifting hydrophilic/hydrophobic mix of the system. This improves hydrophilicity upon polymer degradation and buffers the hydrophobic expansion pressure. This is evident in the decreased swelling caused by the addition of PLGA-acrylate which increases the hydrophobicity of the gel without serving as a crosslink. *In vitro* testing determined the formulations to have suitable mechanical properties and swelling pressure for shape-ability, adequate tissue expansion, and complete removal after expansion.

The mechanical properties, as well as swelling and other properties, are a result of the composition and crosslinking of the hydrogels. The PEG block is more flexible than the PLGA block, and the formulations with high relative contents of PEG (Formulations 1 and 2) have a lower initial elastic modulus. The relaxation (delayed viscous deformation) for the formulations with shorter distances between the crosslinks reflects a higher value as these formulations have very limited capacity for the chains to move relative to each other due to denser crosslinking. All formulations shown, however, had suitable flexibility for reshaping. Some formulations generated with such high crosslinking density exhibited mechanically brittle properties and shattered upon attempts to cut [61]. These formulations were not included in the study.

In vivo model testing indicated that these formulations were well suited for skin application. Throughout the study, only a single event of localized infection was noted. No other localized or systemic toxicity was found. No mechanically-related flap damage such as incision dehiscence, tissue blanching, or necrosis was noted. A key usability feature of the developed expander is its removability. *In vivo* model testing indicated this is an important requirement for the tissue expanding usefulness of the material. By improving the crosslinking density, a formulation was found (Formulation 13) allowing for expander removal as a single piece. Another usability feature is the quality of the expanded tissue. For the tissue to have surgical value, it must be well perfused with oxygenated blood. By maintaining a moderate expansion profile, Formulation 13 allowed for the formation of highly vascularized tissue despite a 2-fold increase in volume under the flap.

5. CONCLUSION

To provide for osmotically powered expansion, without requiring an external membrane, the swelling pressure and rate properties must be built into the hydrogel itself. Such a hydrogel can be generated by use of chemically crosslinked hydrophilic polyether (polyethylene glycol) and hydrophobic polyester (PLGA) wherein the degradation of the PLGA controls the swelling rate. Mechanical properties are maintained by the incorporation of permanent crosslinks of EGDMA to prevent total dissolution of the reshapable hydrogel and to maintain structural integrity in the swollen state. This cohesiveness of the swollen gel allows for surgical removal as one piece without residue in the tissue. Reshapable hydrogels generated in this manner have proven their surgical relevancy in an animal model by the successful expansion of well-vascularized skin in a rat skin model. This technology holds promise for the development of reshapable tissue expanders for clinical use, particularly in physically constrained environments where ability to adjust the expander’s size and shape is desirable.

Acknowledgments

Portions of the research reported in this publication were supported by the National Institute of Health under Award Numbers R43RR024253, R44RR024253, and R44GM106735. A Cooperative Research and Development Agreement (CRADA) existed between Akina, Inc. and Roudebush VA Medical Center, for this study. This material is the result of work supported with resources and the use of facilities at the Richard L. Roudebush VA Medical Center, Indianapolis, Indiana. The content is solely the responsibility of the authors and does not necessarily represent the official views of the National Institutes of Health, the U.S. Department of Veterans Affairs, or the United States Government. Indiana Institute for Medical Research (IIMR) is a non-profit foundation that works to

support and enhance research and development focused on improving the health and quality of life for our nation's Veterans and citizens. The authors want to acknowledge IIMR's support of the work described in this document.

References

1. Neumann CG. The expansion of an area of skin by the progressive distension of a subcutaneous balloon. Plast Reconstr Surg. 1957; 19:124–130.
2. O'Brien CM, Moiemen N. Use of tissue expanders in trauma. Trauma. 2005; 7:69–75.
3. Kobus KF. Cleft palate repair with the use of osmotic expanders: a preliminary report. Journal of Plastic Reconstructive & Aesthetic Surgery. 2007; 60:414–421.
4. Sarkarat, F., Kavandi, F., Kahali, R., Motamedi, MHK. Use of intra-oral osmotic self-inflating tissue expanders for bone reconstruction and rehabilitation of the jaws. In: Motamedi, MHK., editor. A Textbook of Advanced Oral and Maxillofacial Surgery. Vol. 3. InTech; Rijeka: 2016. Ch. 25
5. Asa'ad F, Rasperini G, Pagni G, Rios HF, Gianna AB. Pre-augmentation soft tissue expansion: an overview. Clinical Oral Implants Research. 2015; 27:505–522. [PubMed: 26037472]
6. Acarturk TO, Glaser DP, Newton ED. Reconstruction of difficult wounds with tissue-expanded free flaps. Annals of Plastic Surgery. 2004; 52:493–499. [PubMed: 15096936]
7. Newman R, Cleveland DC. Three-dimensional reconstruction of ultrafast chest CT for diagnosis and operative planning in a child with right pneumonectomy syndrome. CHEST Journal. 1994; 106:973–974.
8. MacLennan SE, Corcoran JF, Neale HW. Tissue expansion in head and neck burn reconstruction. Clinics in Plastic Surgery. 2000; 27:121–132. [PubMed: 10665361]
9. Bauer BS. The role of tissue expansion in reconstruction of the ear. Clinics in Plastic Surgery. 1990; 17:319–325. [PubMed: 2189646]
10. Simpson RL, Flaherty ME. The burned small finger. Clinics in Plastic Surgery. 1992; 19:673–682. [PubMed: 1633674]
11. Silfen R, Hudson DA, Soldin MG, Skoll PJ. Tissue expansion for frontal hairline restoration in severe alopecia in a child. Burns. 2000; 26:294–297. [PubMed: 10741598]
12. Rosselli P, Reyes R, Medina A, Céspedes LJ. Use of a soft tissue expander before surgical treatment of clubfoot in children and adolescents. Journal of Pediatric Orthopaedics. 2005; 25:353–356. [PubMed: 15832154]
13. Pasyk KA, Argenta LC, Austad ED. Histopathology of human expanded tissue. Clin Plast Surg. 1987; 14:435–445. [PubMed: 3301156]
14. Pollard ZF, Greenberg M. Achieving success with the silicone expander for overacting superior obliques. Trans Am Ophthalmol Soc. 1999; 97:333–342. Discussion 342–347. [PubMed: 10703132]
15. Tang Y, Luan J, Zhang X. Accelerating tissue expansion by application of topical papaverine cream. Plast Reconstr Surg. 2004; 114:1166–1169. [PubMed: 15457029]
16. Tucker SM, Sapp N, Collin R. Orbital expansion of the congenitally anophthalmic socket. Br J Ophthalmol. 1995; 79:667–671. [PubMed: 7662633]
17. Gibstein LA, Abramson DL, Bartlett RA, Orgill DP, Upton J, Mulliken JB. Tissue expansion in children: A retrospective study of complications. Annals of Plastic Surgery. 1997; 38:358–364. [PubMed: 9111895]
18. Berge SJ, Wiese KG, von Lindern JJ, Niederhagen B, Appel T, Reich RH. Tissue expansion using osmotically active hydrogel systems for direct closure of the donor defect of the radial forearm flap. Plast Reconstr Surg. 2001; 108:1–5. Discussion 6–7. [PubMed: 11420497]
19. Chummun S, Addison P, Stewart KJ. The osmotic tissue expander: A 5-year experience. Journal of Plastic Reconstructive & Aesthetic Surgery. 2010; 63:2128–2132.
20. Swan MC, Bucknall DG, Goodacre TEE, Czernuszka JT. Synthesis and properties of a novel anisotropic self-inflating hydrogel tissue expander. Acta Biomaterialia. 2011; 7:1126–1132. [PubMed: 20971218]
21. Wysocki M, Kobus K, Szotek S, Kobielarz M, Kuropka P, Będziński R. Biomechanical effect of rapid mucoperiosteal palatal tissue expansion with the use of osmotic expanders. Journal of Biomechanics. 2011; 44:1313–1320. [PubMed: 21295780]

22. Maxwell, GP., Gabriel, A. The development of breast implants. In: Peters, W.Brandon, H.Jerina, KL.Wolf, C., Young, VL., editors. Biomaterials in Plastic Surgery. Woodhead Publishing; 2012. p. 40-51.
23. Chhaya, MP., Melchels, FPW., Wiggenhauser, PS., Schantz, JT., Hutmacher, DW. Breast reconstruction using biofabrication-based tissue engineering strategies. In: Forgacs, G., Sun, W., editors. Biofabrication. William Andrew Publishing; Boston: 2013. p. 183-216.Chapter 110
24. Maitz MF. Applications of synthetic polymers in clinical medicine. Biosurface and Biotribology. 2015; 1:161–176.
25. Rees L, Morris P, Hall P. Osmotic tissue expanders in cleft lip and palate surgery: a cautionary tale. Journal of Plastic, Reconstructive & Aesthetic Surgery. 2008; 61:119–120.
26. Ethicon. Coated VICRYL® (polyglactin 910) Suture. 2016. http://www.ethicon.com/healthcare-professionals/products/wound-closure/absorbable-sutures/coated-vicryl-polyglactin-910-suture
27. Makadia HK, Siegel SJ. Poly lactic-co-glycolic acid (PLGA) as biodegradable controlled drug delivery carrier. Polymers. 2011; 3:1377–1397. [PubMed: 22577513]
28. Anderson JM, Shive MS. Biodegradation and biocompatibility of PLA and PLGA microspheres. Adv Drug Del Rev. 2012; 64:72–82.
29. Harris, JM. Poly(Ethylene Glycol) Chemistry: Biotechnical and Biomedical Applications. Plenum Publishing; New York, NY: 1992. p. 385
30. Huh, KM., Choi, YM., Park, JH., Park, K. Readily shapeable xerogels having controllably delayed swelling properties. US 2007/0031499 A1. 2007.
31. Tran, TH., Garner, J., Fu, Y., Park, K., Huh, KM. Biodegradable elastic hydrogels for tissue expander application. In: Lendlein, A., Sisson, A., editors. Handbook of Biodegradable Polymers: Isolation, Synthesis, Characterization and Applications. Wiley-VCH; Weinheim, Germany: 2011. p. 217-236.Chapter 219
32. Yuk KY, Kim YT, Im SJ, Garner J, Fu Y, Park KN, Park JS, Huh KM. Preparation and Characterization of Biodegradable Hydrogels for Tissue Expander Application. Polymer Korea. 2010; 34:253–260.
33. Dechy-Cabaret O, Martin-Vaca B, Bourissou D. Controlled ring-opening polymerization of lactide and glycolide. Chemical Reviews. 2004; 104:6147–6176. [PubMed: 15584698]
34. Asandei AD, Erkey C, Burgess DJ, Saquing C, Saha G, Zolnik BS. Preparation of drug delivery biodegradable PLGA nanocomposites and foams by supercritical CO2 expanded ring opening polymerization and by rapid expansion from CHCIF2 supercritical solutions. Mater Res Soc Symp Proc. 2005; 845:243–248.
35. Yu L, Zhang H, Ding J. Effects of precipitate agents on temperature-responsive sol-gel transitions of PLGA-PEG-PLGA copolymers in water. Colloid and Polymer Science. 2010; 288:1151–1159.
36. Lih E, Joung YK, Bae JW, Park KD. An in situ gel-forming heparin-conjugated PLGA-PEG-PLGA copolymer. Journal of Bioactive and Compatible Polymers. 2008; 23:444–457.
37. Feng Y, Zhang S, Zhang L, Guo J, Xu Y. Synthesis and characterization of hydrophilic polyester-PEO networks with shape-memory properties. Polymers for Advanced Technologies. 2011; 22:2430–2438.
38. Fernandez-Carballido A, Puebla P, Herrero-Vanrell R, Pastoriza P. Radiosterilisation of indomethacin PLGA/PEG-derivative microspheres: Protective effects of low temperature during gamma-irradiation. Int J Pharm. 2006; 313:129–135. [PubMed: 16495023]
39. Hausberger AG, Kenley RA, DeLuca PP. Gamma irradiation effects on molecular weight and in vitro degradation of poly (D, L-lactide-co-glycolide) microparticles. Pharm Res. 1995; 12:851–856. [PubMed: 7667189]
40. Montanari L, Cilurzo F, Valvo L, Faucitano A, Buttafava A, Groppo A, Genta I, Conti B. Gamma irradiation effects on stability of poly (lactide-co-glycolide) microspheres containing clonazepam. J Control Release. 2001; 75:317–330. [PubMed: 11489319]
41. Jo SY, Park JS, Gwon HJ, Shin YM, Khil MS, Nho YC, Lim YM. Degradation behavior of poly (L-lactide-co-glycolide) films through gamma-ray irradiation. Radiation Physics and Chemistry. 2012; 81:846–850.
42. Sargeant TD, Desai AP, Banerjee S, Agawu A, Stopek JB. An in situ forming collagen-PEG hydrogel for tissue regeneration. Acta Biomaterialia. 2012; 8:124–132. [PubMed: 21911086]

43. Csima G, Vozary E. Stretched exponent rheological model of gum candy. Acta Alimentaria. 2016; 45:149–156.
44. Kemp, W. Organic Spectroscopy. 3rd. Palgrave; 1991. p. 416
45. Speight, JG. Lange's Handbook of Chemistry, 70th Anniversary Edition. 16th. McGraw-Hill; New York, NY: 2005. p. 1608
46. Mohan, J. Organic Spectroscopy: Principles and Applications. 2nd. CRC Press; Boca Raton, FL: 2004. p. 563
47. Agilent. Polymer molecular weight distribution and definitions of mw averages. 2015. https://www.agilent.com/cs/library/technicaloverviews/Public/5990-7890EN.pdf
48. Wiese, KG. Tissue expander inflating due to osmotic driving forces of a shaped body of hydrogel and an aqueous solution. US 5,496,368. 1996.
49. Gu, K. Tissue expander inflating due to osmotic driving forces of a shaped body of hydrogel and an aqueous solution. US 5,496,368 A. 1996.
50. Min Z, Svensson H, Svedman P. On expander pressure and skin blood flow during tissue expansion in the pig. Ann Plast Surg. 1988; 21:134–139. [PubMed: 3178120]
51. Fu K, Pack DW, Klibanov AM, Langer R. Visual evidence of acidic environment within degrading poly (lactic-co-glycolic acid)(PLGA) microspheres. Pharm Res. 2000; 17:100–106. [PubMed: 10714616]
52. Zolnik BS, Burgess DJ. Effect of acidic pH on PLGA microsphere degradation and release. J Control Release. 2007; 122:338–344. [PubMed: 17644208]
53. Pietila JP, Nordstrum RE, Virkkunen PJ, Voutilainen PE, Rintala AE. Accelerated tissue expansion with the "overfilling" technique. Plastic and Reconstructive Surgery. 1988; 81:204–207. [PubMed: 3336651]
54. Duan H, Gu S, Zhao L, Lu D. Establishment of fracturability standard reference scale by instrumental and sensory analysis of Chinese food. Journal of Texture Studies. 2014; 45:148–154.
55. Santana P, Huda N, Yang TA. The addition of hydrocolloids (carboxymethylcellulose, alginate and konjac) to improve the physicochemical properties and sensory characteristics of fish sausage formulated with surimi powder. Turkish Journal of Fisheries and Aquatic Sciences. 2013; 13:561–569.
56. Boodhoo M, Humphrey K, Narine S. Relative hardness of fat crystal networks using force displacement curves. International Journal of Food Properties. 2009; 12:129–144.
57. Bakker D, Blitterswijk CV, Hesseling S, Grote J, Daems WT. Effect of implantation site on phagocyte/polymer interaction and fibrous capsule formation. Biomaterials. 1988; 9:14–23. [PubMed: 2832011]
58. Swan MC, Bucknall DG, Czernuszka JT, Pigott DW, Goodacre TEE. Development of a novel anisotropic self-inflating tissue expander: In vivo submucoperiosteal performance in the porcine hard palate. Plast Reconstr Surg. 2012; 129:79–88. [PubMed: 22186501]
59. Wiese KG, Heinemann DE, Ostermeier D, Peters JH. Biomaterial properties and biocompatibility in cell culture of a novel self-inflating hydrogel tissue expander. J Biomed Mater Res. 2001; 54:179–188. [PubMed: 11093177]
60. Ronert MA, Hofheinz H, Manassa E, Asgarouladi H, Olbrisch RR. The beginning of a new era in tissue expansion: self-filling osmotic tissue expander—four-year clinical experience. Plast Reconstr Surg. 2004; 114:1025–1031. [PubMed: 15457009]
61. Barco, CT., Park, K., Park, H., Fu, Y., Garner, JS. Novel hydrogel tissue expanders. PCT/US2015/025556. 2015.

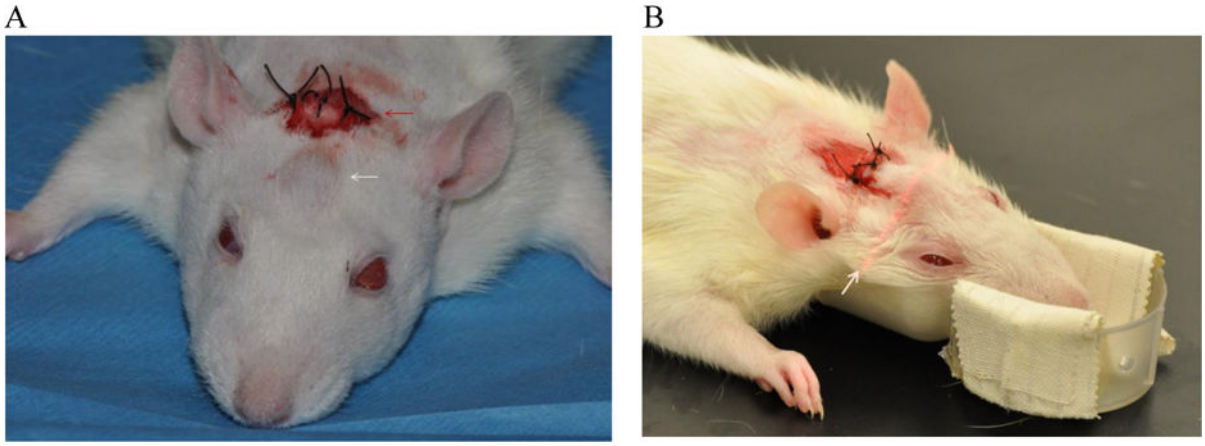

Fig. 1.

(A) Rat head immediately after implantation surgery with sutures (red arrow). The implanted gel is indicated by a white arrow. (B) The swelling of an implanted gel over time is measured by laser scanning. The pink arrow shows a laser scanning line.

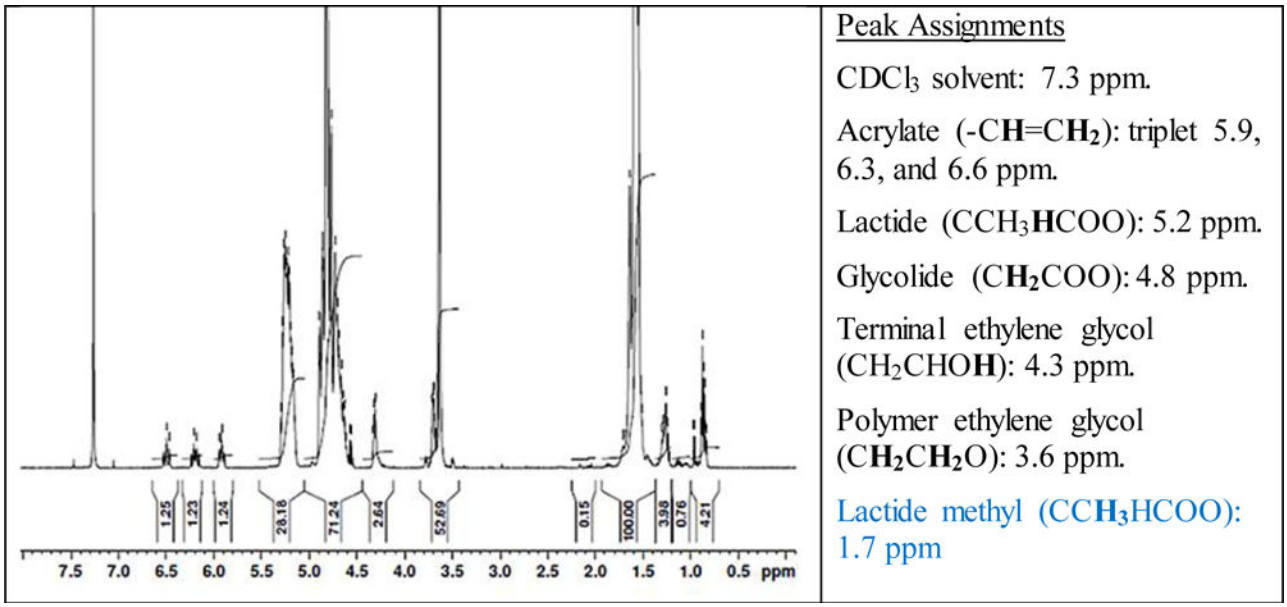

Fig. 2.

NMR analysis of a synthesized triblock PLGA-PEG-PLGA diacrylate with block molecular weights of 5,000-1,000-5,000 (M2 in Table 1).

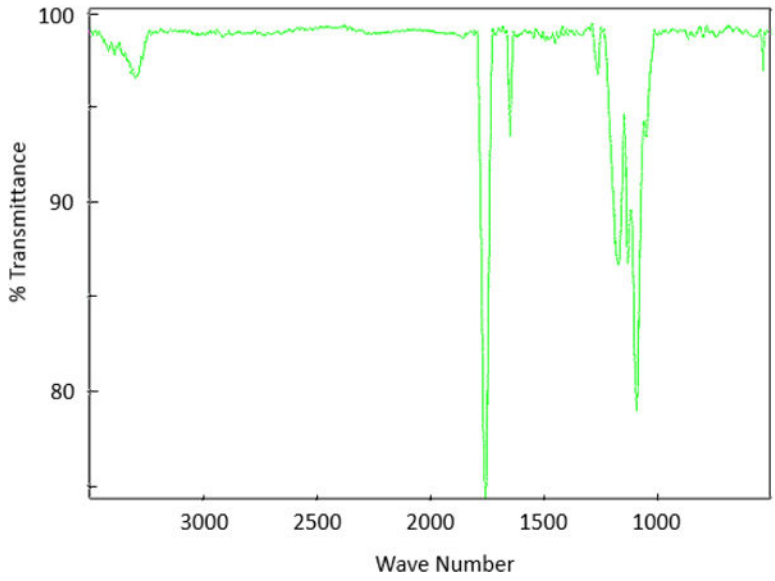

Fig. 3.
FTIR spectrum of PLGA-PEG-PLGA diacrylate (M2 in Table 1).

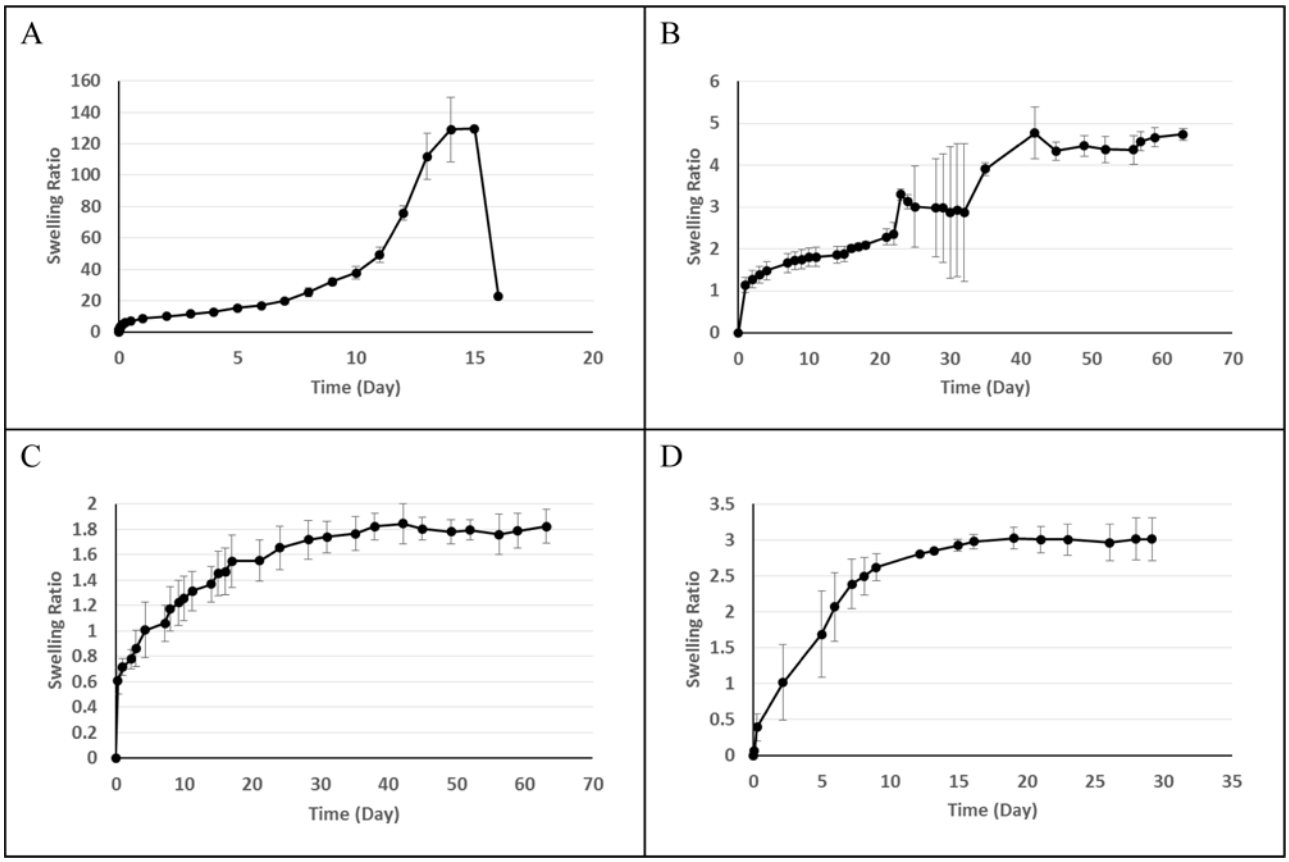

Fig. 4.

In vitro swelling profile of Formulations 1 (A), 3 (B), 13 (N = 12) (C), and Osmed (D). Error bars show standard deviation. Unless otherwise specified, N = 3.

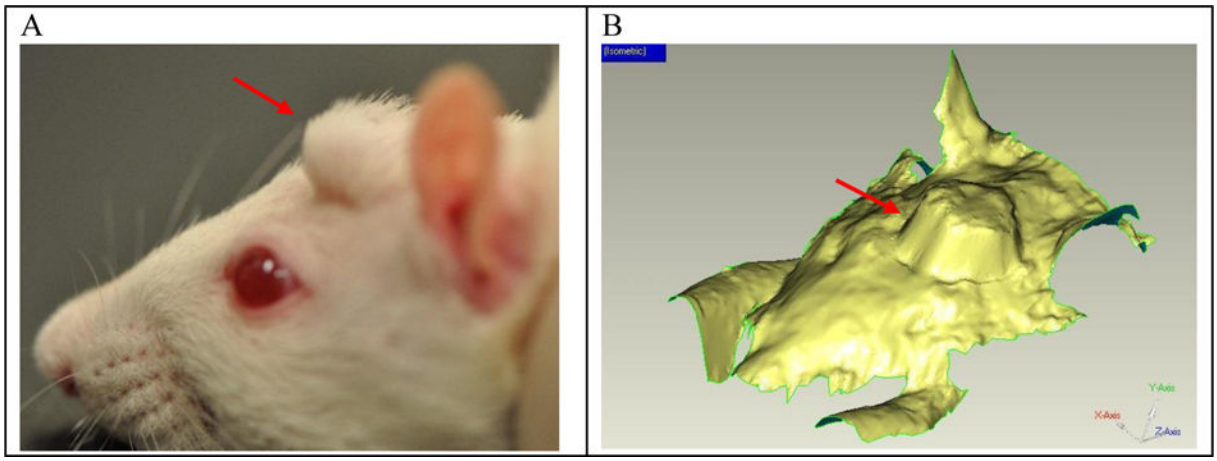

Fig. 5.

A side profile view of a rat with an expander implanted in the head (A) and an image of 3D scan data from rat used in 3D analysis testing (B). The red arrow indicates the location of the implanted expander.

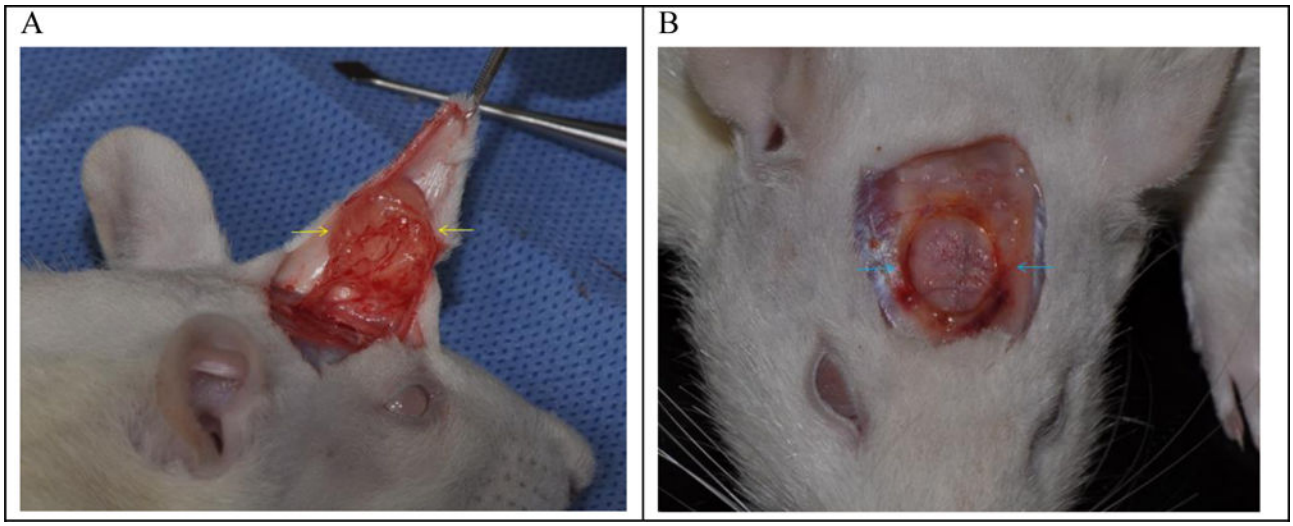

Fig. 6.

(A) A hydrogel tissue expander (Formulation 8 in Table 3) wrapped around by a formed fibrous capsule (yellow arrows) after 6 weeks of insersion. (B) Another tissue exander showing slight resorotion of bone (blue arrows) due to expanding gel.

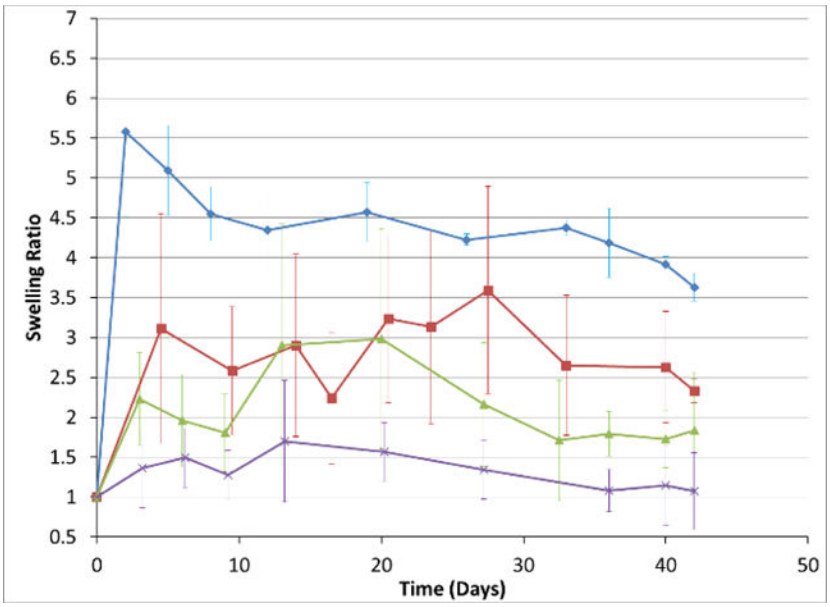

Fig. 7.

In vivo volume expansion profiles of Osmed (Blue diamond), Formulation 5 (red square), Formulation 12 (green triangle) and Formulation 13 (purple x). (Average ± standard deviation).

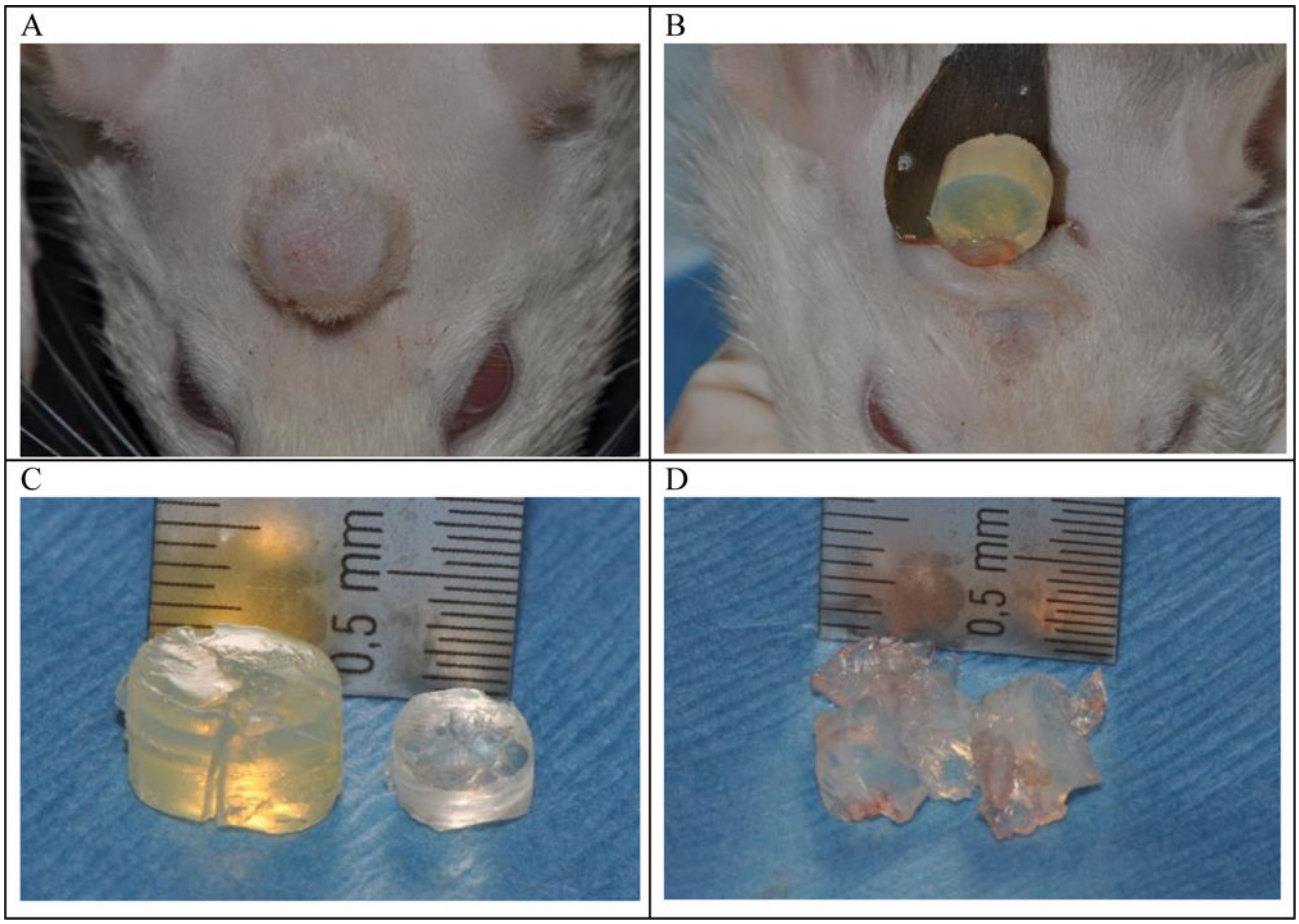

Fig. 8.

Swelling of Formulation 13 for 6 weeks on a rat head (**A**). Removal of the swollen Formulation 13 after incision through the skin (**B**). Comparison of the recovered Formulation 13 (left) and the original hydrogel before implantation (right) (**C**). Removal of the swollen Formulation 12 from tissue for comparison (**D**).

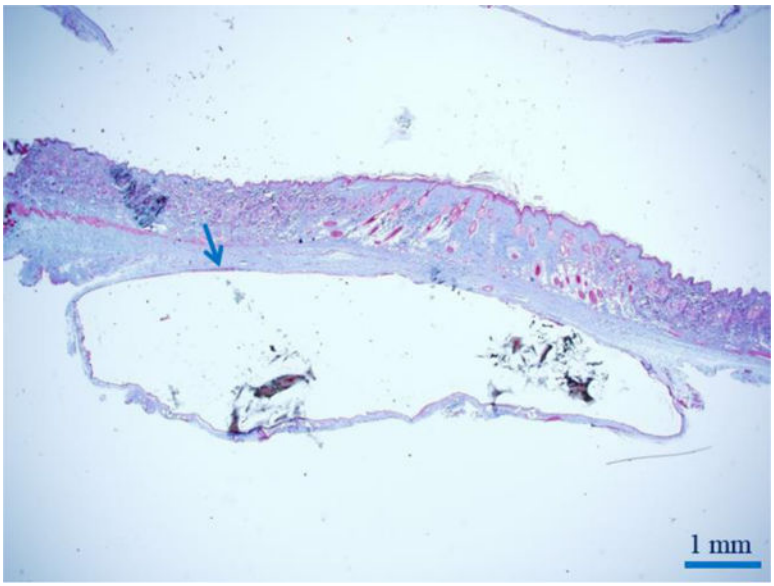

Fig. 9.

Trichrome stain of the inner fibrous capsule (blue arrow) by skin during rat study. A capsule consistently formed around the expanded reshapable hydrogel.

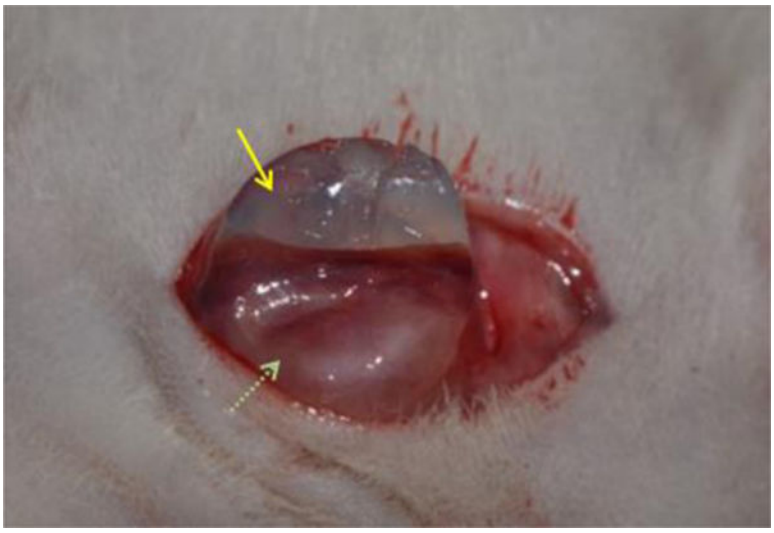

Fig. 10.
Hydrogel (yellow arrow) enveloped in fibrous capsule (green dotted arrow) at removal.

Table 1

Acrylate activated triblock PLGA-PEG-PLGA copolymers.

Macromer Code	Description
M1	PLGA-PEG-PLGA diacrylate (L:G 50:50) 333-1500-333 Da
M2	PLGA-PEG-PLGA diacrylate (L:G 50:50) 5000-1000-5000 Da
M3	PLGA-PEG-PLGA diacrylate (L:G 50:50) 7500-1000-7500 Da
M4	PLGA acrylate (L:G 50:50) 20,000 Da
M5	PLGA-PEG-PLGA diacrylate (L:G 80:20) 492-1500-492 Da

Table 2

GPC data from a series of different lots of **M2.**

Lot#	Molecular Weight		PDI
	Number average (Da)	Weight average (Da)	
1	9,180	18,848	2.05
2	8,458	17,729	2.10
3	10,276	15,792	1.54

Table 3

Reshapable hydrogel formulations used in this research.

Formulation	Hydrogel composition (%(w/w) specified macromers)
1	50.0% M1 + 50.0% PEGDA (700 Da)
2	66.6% M5 + 33.3% PEGDA (700 Da)
3	60.6% M2 + 30.3% PEGDA (700 Da) + 9.1% M4
4	70.2% M2 + 26.3% PEGDA (700 Da) + 3.5% M4
5	45.1% M2 + 48.4% PEGDA (700 Da) + 6.4% M4 + 0.1% EGDMA
6	60.5% M2 + 30.3% PEGDA (700 Da) + 9.1% M4 + 0.1% EGDMA
7	63.2% M2 + 31.6% PEGDA (700 Da) + 4.8% M4 + 0.5% EGDMA
8*	60.6% M2 + 30.3% PEGDA (700 Da) + 9.1% M4
9	58.0% M3 + 29.0% PEGDA (700 Da) + 8.7% M4 + 4.3% EGDMA
10	69.9% M3 + 26.2% PEGDA (700 Da) + 3.8 % EGDMA
11	60.7% M2 + 26.6% PEGDA (700 Da) + 8.4% M4 + 4.2% EGDMA
12	40.0% M2 + 42.8% PEGDA (700 Da) + 17.2% M4 + 0.1% EGDMA
13	39.3% M2 + 42.1% PEGDA (700 Da) + 5.6% M4 + 12.9 % EGDMA
Osmed	Methyl methacrylate and N-vinylpyrrolidone copolymer (Periost Expander 0.45 ml)

* Dip coated with poly(N-vinylpyrrolidinone) (PVP) (55,000 Da).

Table 4

Mechanical properties of dry reshapable hydrogels (average ± standard deviation).

Formulation	Elastic modulus (kPa)	Stress Relaxation (%)	Swelling pressure (mmHg)
1	2 ± 0.5 (n=3)	94 ± 0.3 (n=3)	450 ± 87 (n=3)
2	2 ± 1 (n=3)	95 ± 1 (n = 3)	1,614 ± 560 (n=3)
13	10 ± 6 (n=12)	52 ± 5 (n=12)	794 ± 362 (n=12)

Table 5

End-strength of swollen hydrogels after 2-month incubation at 37 °C in PBS. Data shown as average ± standard deviation.

Formulation	End-Strength
1	Dissolves to liquid after 16 days (n=3)
2	0.05 ± 0.05 N/mm (n=3)
9	0.02 ± 0.003 N/mm (n=2)
10	0.18 ± 0.11 N/mm (n=2)
11	0.07 N/mm (n=1)
12	0.42 N/mm (n=1)
13	0 N/mm (n=3)

Table 6

The *in vivo* volume swelling change (ΔV_t) as measured by Faro® arm.

Formulation	Swelling (Average volume change)		
	Day 2	Day 15	Day 42
3	1.37 ± 0.27 *	1.78 ± 0.47 *	1.65 ± 0.02 *
4	1.50 ± 0.30	2.42 ± 0.44	1.79 ± 0.40
5	1.65 ± 0.09	2.22 ± 0.65	1.89 ± 0.28
6	1.48 ± 0.28	2.33 ± 0.35	2.87 ± 1.01
7	1.49 ± 0.47	1.75 ± 0.61	1.66 ± 0.08
8	1.36 ± 0.20	1.08 ± 0.85	1.74 ± 1.34

Average ± standard deviation

*(N = 2, otherwise N=3)